



Photo Credits: Ann Bishop - The Cultured Abalone Farm

Modelling Data-Poor Species for Fisheries Management: The Story of Northern California Red Abalone, *Haliotis rufescens*

Eva Juengling Bean¹, Daniel O'Shea²

juenglingbean@bren.ucsb.edu, oshea@ucsb.edu

Eva Juengling Bean, Daniel O'Shea. 2026. Modelling Data-Poor Species for Fisheries Management: The Story of Northern California Red Abalone, *Haliotis rufescens*. In: Population Ecology in Practice: Modelling and Storytelling in a Changing World, edited by C.L. Jerde. University of California, Santa Barbara. This work is licensed under Creative Commons Attribution 4.0 International License (CC BY 4.0).

Preferred citation: Juengling Bean, E. J. and O'Shea, D. C. (2026). Modelling Data-Poor Species for Fisheries Management: The Story of Northern California Red Abalone, *Haliotis rufescens*. In C. L. Jerde (Ed.), Population Ecology in Practice: Modelling and Storytelling in a Changing World. University of California, Santa Barbara. CC BY 4.0. (pp. [XXX-XXX]).

What will you learn from this?

- How to graphically reduce a Life History Matrix and calculate R_0 .
- Use an R_0 function to visualize population growth after perturbations.
- Compare R_0 outputs to real-life data to identify trends.
- **Keywords:** matrix models, net reproductive rate, graph reduction, harvest pressure, marine heatwave, fecundity
- **Related chapters:**
 - House of the Rising Sunflower Seastar: Modeling *Pycnopodia helianthoides* home ranges to explore recovery patterns.
 - Cutthroat Competition
 - Matrix Models and Wild Rice (*Zizania palustris*) in the Midwestern U.S.

Background

Red abalone (*H. rufescens*) are the largest species of abalone in the world and are only found along the coast of California (Ault, 1985). *H. rufescens* inhabit subtidal and intertidal kelp forests to depths of 100 feet and eat a variety of algae species (Ault, 1985). These abalone spawn in spring and early summer through broadcast spawning and fertilize their eggs externally. The maturation of the abalone gonad is heavily dependent on the quality and quantity of the surrounding algae that they feed on (Ault, 1985). As abalone spawn, their eggs, and subsequently sperm, settle at the bottom of the seafloor. Lecithotrophic

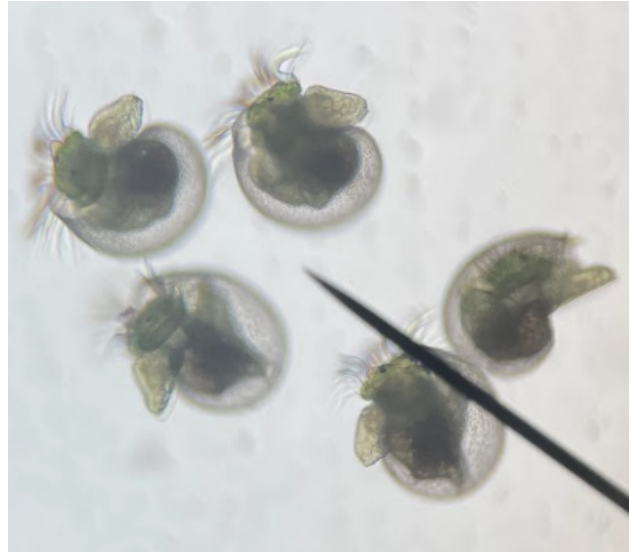


Image 1; Abalone Veligers. Photo Credits: Ann Bishop - The Cultured Abalone Farm

trochophore larvae generally begin to emerge from the eggs about 10-12 hours after fertilization, then become more mobile veliger larvae that settle on their preferred cryptic coralline algae substrate after 5 to 14 days (Ault, 1985). At this point in their development, the post-larval abalone subsist on bacteria

and diatoms until they reach 10mm. At this size class, the abalone begin to graze on different macroalgae species, begin to grow their characteristic ear-shaped shell, and open new respiratory holes while closing older holes. Interestingly, *H. rufescens* are seldom seen before they are 100mm (Ault, 1985). Growth at this point continues at a steady rate defined in part by the temperature of the surrounding waters and the quality of algae around them. Abalone at 100mm are generally 4 years old. *H. rufescens* reach a maximum size of 290 mm and have been observed growing approximately 50 mm per year in Central California (Ault, 1985). Growth rates vary seasonally, reflecting the amount of nearby food (brown algae). In Northern California, where the predominant canopy-forming kelp species is the annual *Nereocystis lutea*, 80% of *H. rufescens* growth occurs during the summer months (Ault, 1985).

Overall, *H. rufescens* veligers (Image 1) are heavily dependent on the availability of brown algae where they settle, as it provides a more cryptic benthic environment and high-quality food that drives more efficient growth and gonadal development. Temperature also plays a major role in the development and survival of larval abalone, along with competition from other herbivores such as the purple and red urchins, *Strongylocentrotus purpuratus* and *Mesocentrotus franciscanus*, which also graze on drift brown algae in similar rocky subtidal habitats (Ault, 1985; Braje et al., 2009). Juvenile *H. rufescens* feed predominantly on diatom films or other microscopic algae, while adults feed on brown macroalgae (Ault, 1985).

Adult abalone are primarily preyed upon by *Enhydra lutris*, the sea otter, and by a host of other species when they are juveniles (Braje et al., 2009). Predation from Native Californians was also influential in controlling abalone populations (Braje et al., 2009). When both otter and Native Californian predation pressure were released in the 1800s, populations of abalone and urchin skyrocketed (Braje et al., 2009). Since then, the abalone fishery has historically been one of the state's most economically significant fisheries both commercially and recreationally. With this much pressure, there have been multiple periods of decline due to overfishing, El Niño events, kelp loss, and competition with urchins, which we will discuss in more detail. Modern recreational fishing for *H. rufescens* between 2002 and 2014 averaged 35,000 fishers taking 245,000 *H. rufescens* per year, with 95% of that catch coming from Sonoma and Mendocino counties in Northern California (Reid et al., 2016). Economically, estimates from 2013, based on data from 31,000 fishers, found that the red abalone fishery generated \$24M to \$44M in recreational value per year (Reid et al., 2016). Since the more recent closures, communities in Northern California have been heavily impacted by the loss of tourism. Our study area will continue to combine life-history information with fisheries modeling to help Northern California abalone

populations rebound, while also expanding fishing opportunities to increase economic activity in the area surrounding the recreational red abalone fishery.

H. rufescens has been a vital resource in Northern California for generations, serving as both a cultural symbol and a food source for Indigenous and coastal California communities. Historically supporting both recreational and commercial fishing activity in Sonoma and Mendocino Counties, the red abalone fishery has been actively managed since the middle of the 19th century (CDFW, 2003). After decades of large-scale commercial landings led to population dips, the California Department of Fish and Wildlife (CDFW) closed the commercial fishery in 1997. The recreational fishery north of San Francisco persisted until 2018, when abalone populations decreased drastically, prompting a recreational shutdown until 2036 (CDFW, 2025).

Several factors contributed to the closure of the recreational fishery. Rising sea surface temperatures (SSTs) reduced the availability of vital nutrients for algal species that are often abundant in cold-water upwelling zones. The Blob, a marine heat wave (MHW) that occurred off the North Coast of California in 2014, prevented the successful recruitment and growth of algal species that *H. rufescens* rely on throughout their life stages. This contributed to the large-scale kelp die-off that is still prevalent in North Coast waters. On top of that, the spread of sea star wasting disease in Northern California decimated sunflower star populations, a primary predator of purple and red sea urchins. Without predatory pressure, urchin populations boomed, often outcompeting abalone for kelp resources that were already limited (CDFW, 2016). As a result, *H. rufescens* populations declined by 85%, prompting concerns about local extinction (CDFW, 2025). Abalone's reproductive strategy, broadcast spawning, relies on high local densities to encourage successful external fertilization, as discussed above. When densities fall to a certain level, abalone become uniquely vulnerable to Allee effects, where individual fitness decreases drastically at small population sizes or low local density.

These population concerns are complicated further by limited public data availability. CDFW regularly surveys within *H. rufescens* ranges to inform ongoing fishery decisions, but due to poaching concerns, much of this data is difficult to access. Scientific studies have worked to model population growth, fecundity, and mortality rates since the early 2000s, but there has been limited insight into the relationship between fishing pressure and abalone population success for future management (Rogers-Bennett, 2006; Rogers-Bennett, 2007; Rogers-Bennett, 2013; Rogers-Bennett & Dondaville, 2016; Virgin, 2025). Our modeling approach below uses historical catch, fecundity, growth, and mortality data to assess the growth rates of modern *H. rufescens* populations under different fishing

scenarios. Although rife with uncertainty, this framework may be of use in supporting a general understanding of fisheries models, particularly for data-limited species. The study areas that defined our model are shown in Figure 1.

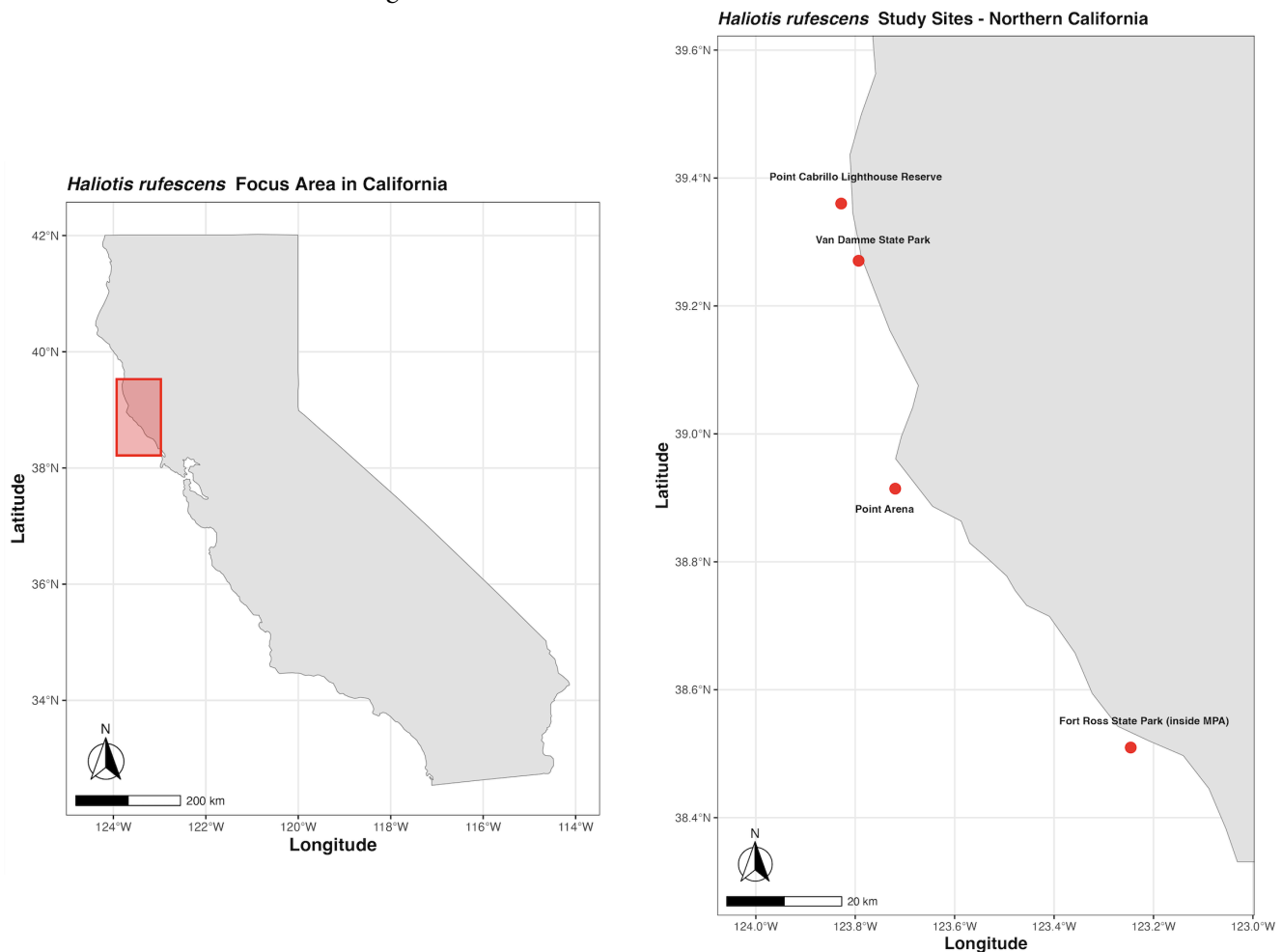


Figure 1: General study area and study sites for Northern California *H. rufescens* population modelling.

Data

Survey-level, modern data regarding North Coast *H. rufescens* populations were difficult to obtain within the time constraints of this effort. Data limitations, therefore, informed the chapter's conceptual direction. The most consequential piece of data for the modelling approach is the *H. rufescens* population matrix, sourced from Rogers-Bennett & Leaf (2006; Table 1). All data used, their citations, and hyperlinks are available in Table 2.

Table 1: *H. rufescens* life history matrix, including survivorship probabilities and fecundities, as described in Rogers-Bennett & Leaf, 2006. The top row of data represents the relative fecundities of each reproductively viable size class (size class columns 4-8).

Size Class (Shell Length, mm)	Transition size class (Shell Length, mm)							
	25-50	50.1-75	75.1-100	100.1-125	125.1-150	150.1-178	178-200	>200.1
25-50	0.191	0.000	0.000	0.800	3.790	12.33	24.02	30.33
50.1-75	0.191	0.045	0.000	0.000	0.000	0.000	0.000	0.000
75.1-100	0.000	0.360	0.148	0.000	0.000	0.000	0.000	0.000
100.1-125	0.000	0.045	0.342	0.180	0.000	0.000	0.000	0.000
125.1-150	0.000	0.000	0.037	0.405	0.321	0.000	0.000	0.000
150.1-178	0.000	0.000	0.000	0.013	0.343	0.67	0.048	0.000
178.1-200	0.000	0.000	0.000	0.000	0.000	0.06	0.726	0.010
>200.1	0.000	0.000	0.000	0.000	0.000	0.000	0.010	0.735

Table 2: Data utilized for modelling objectives.

Data Citation	Description	Hyperlink
Rogers-Bennett, L., Leaf, R. T. (2006). Elasticity analyses of size-based red and white abalone matrix models: Management and conservation. Ecological Society of America: Ecological Applications, 16(1), 213-224.	Peer reviewed literature containing population matrix data and describing relevant methods	https://doi.org/10.1890/04-1688
Rogers-Bennett, L. (2025). Lengths of organisms recorded during emergent and rapid emergent surveys conducted in the subtidal zone of northern California, Sonoma and Mendocino counties, from 1999 to 2023. Biological and Chemical Oceanography Data Management Office (BCO-DMO). (Version 1) Version Date 2024-06-04. doi:10.26008/1912/bco-dmo.929286.1 [March 2, 2026]	Data from long-term CDFW emergent dive surveys across Northern California sites. Data monitors sizes and counts of abalone, urchin, and kelp species.	bull_kelp_survey_data

Modelling Approaches

As cited above, the basis of this model was a population matrix described in Rogers-Bennett & Leaf (2006). Matrix models can be useful tools to describe survivorship probabilities between explicitly defined life stages. **Fecundity**, or the number of reproductively-viable offspring a reproductively-viable individual of a given life stage will contribute to the population, is also described within a matrix.

Matrix models can address issues in both conservation and management, but require large amounts of data to draw confident conclusions and projections (Caswell, 2001). Matrix-based **sensitivity** and **elasticity** analyses can help determine which life stage contributes most to a given population's persistence (de-Camino-Beck & Lewis, 2008; Caswell, 2019; Jones, 2026). In addition, traditional matrix models can be used to project population age distributions over a short period. To achieve this, however, survey-level data describing population numbers at each life stage are necessary (Jones, 2026). Because our access to such data was limited, we decided to pursue a deterministic mathematical model that could be developed from the published population matrix to visualize *H. rufescens* population change under different scenarios.

The best way to illustrate such population change was to calculate the Net Reproductive Rate (NRR or R_0). R_0 , a term derived from stage-specific fecundity contributions, is defined as the average number of offspring a reproductively-viable individual will contribute to the population in their lifetime. Thus, R_0 can be used as a proxy for population growth rate (λ) (de-Camino-Beck & Lewis, 2008). An R_0 value larger than 1 implies population growth ($\lambda > 0$), while an R_0 value less than 1 implies population decline ($\lambda < 0$). An R_0 value exactly equal to 1 describes a population in which each reproducing individual contributes 1 offspring to the population on average, implying no population growth ($\lambda = 0$).

To calculate the R_0 of *H. rufescens* on California's North Coast, we graphically represented the published population matrix and derived an R_0 equation using graph reduction methodology (de-Camino-Beck & Lewis, 2008). This methodology is built around three reduction rules, as described in Figure 2.

Using these rules, the published *H. rufescens* population matrix was graphically represented and then reduced according to the steps outlined in Figure 3. For figure clarity, size-based life stages were represented with single numbers. Stage numbers as depicted in the stepwise graph reduction are matched with their respective size classes in the Supplemental Materials (Supplemental Table 1).

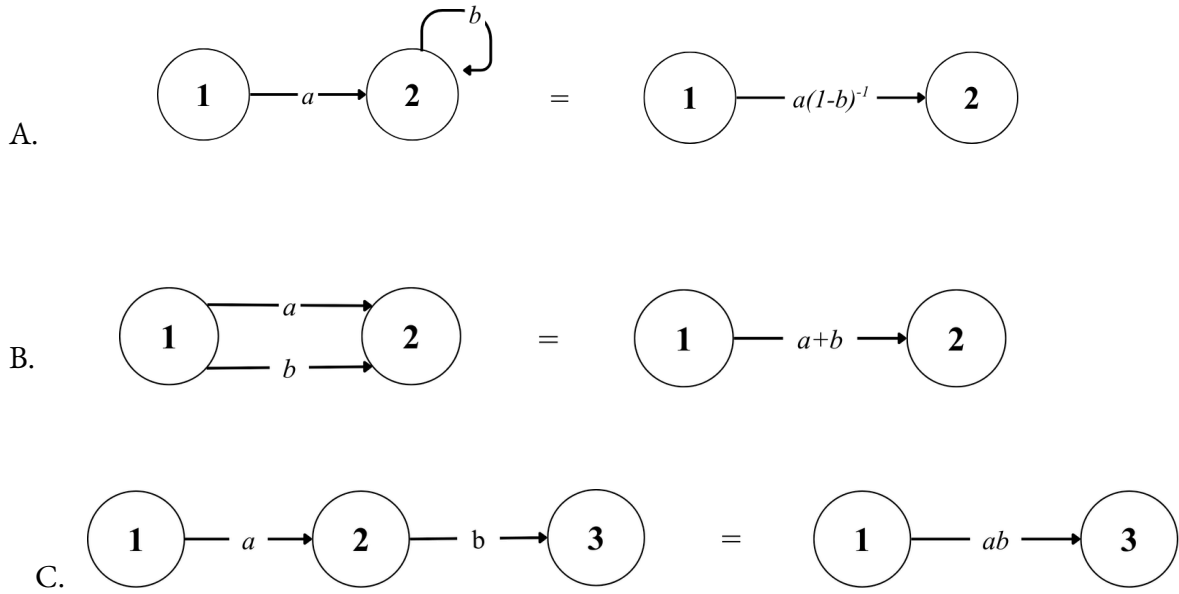
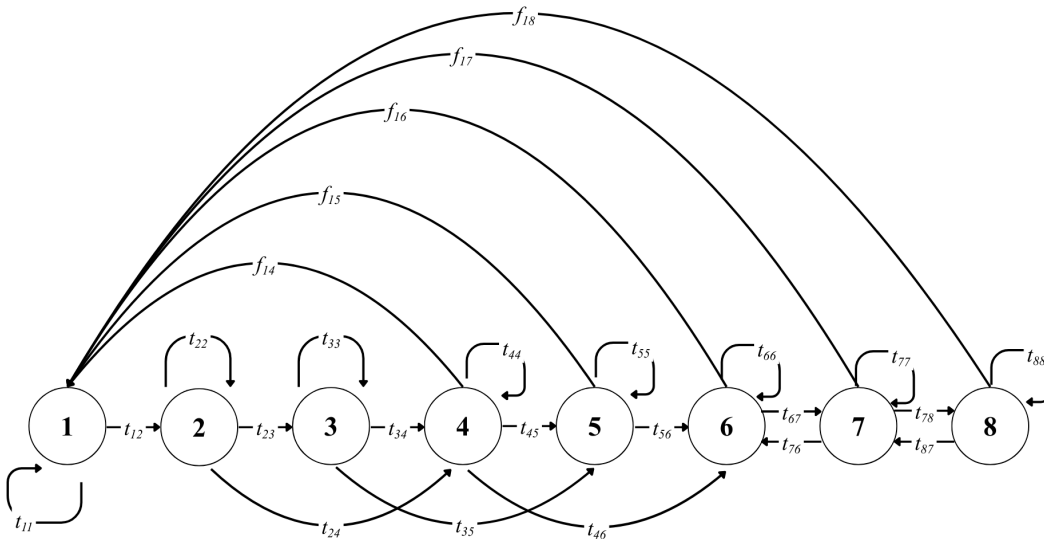
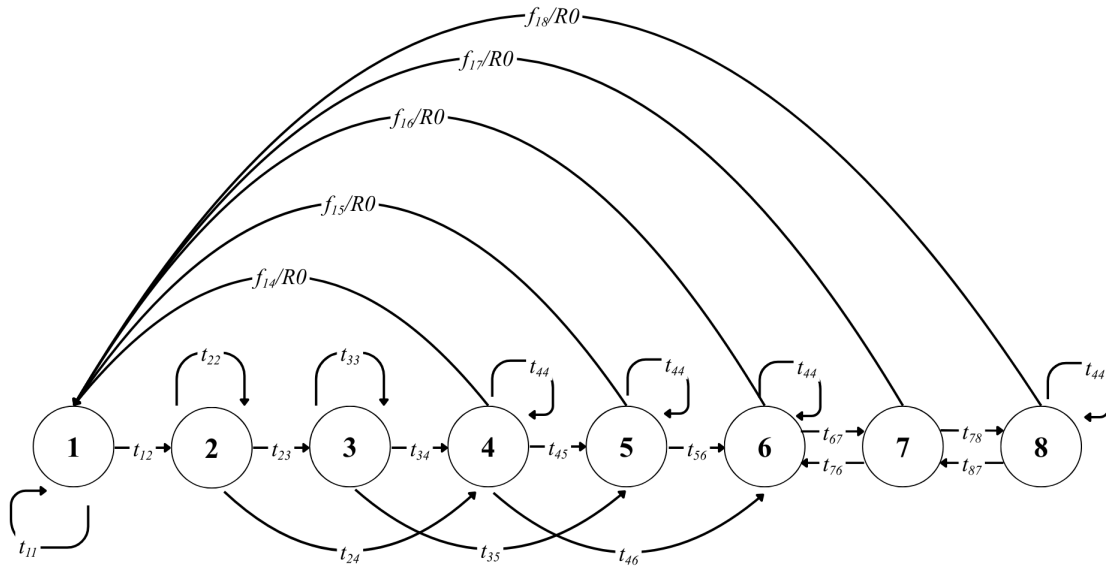


Figure 2: Graph reduction rules (de-Camino-Beck & Lewis, 2008). These rules informed the graph reduction of the *H. rufescens* population matrix.

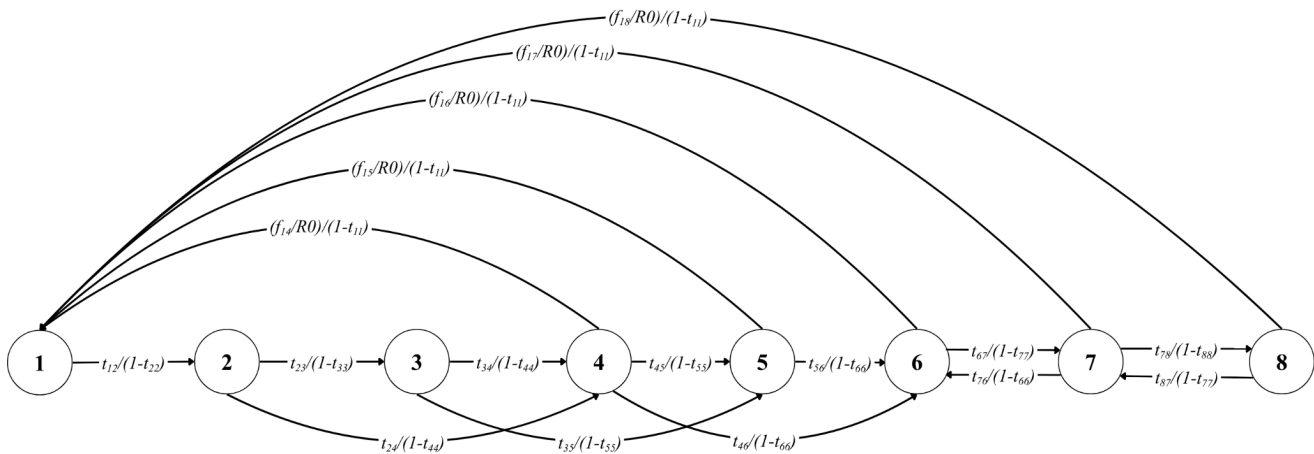
1. Graphical representation of *H. rufescens* population matrix



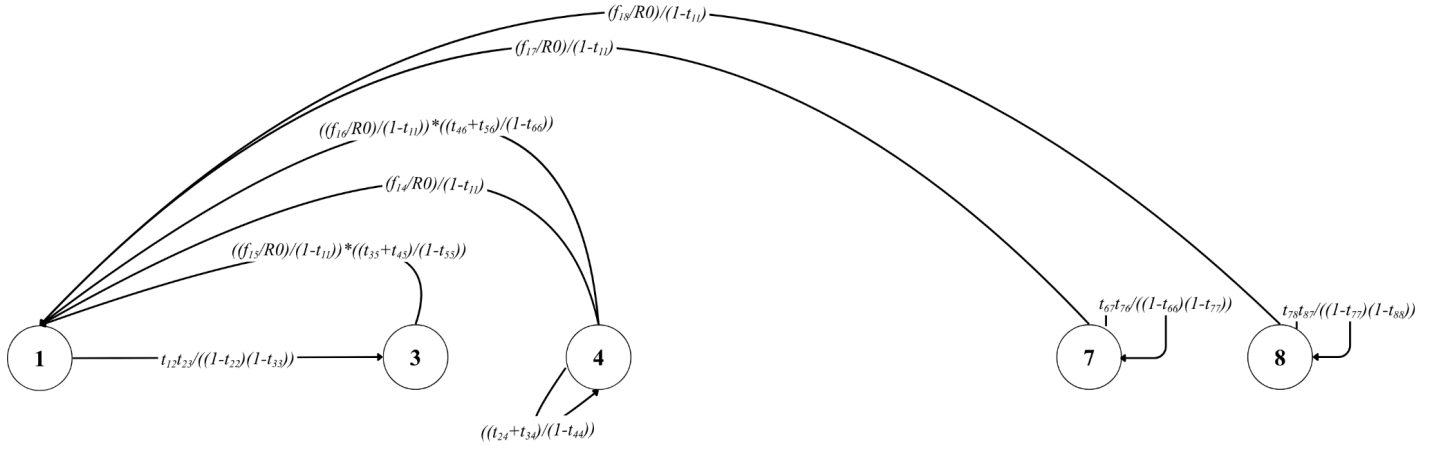
2. Divide all fecundities by R_0 variable



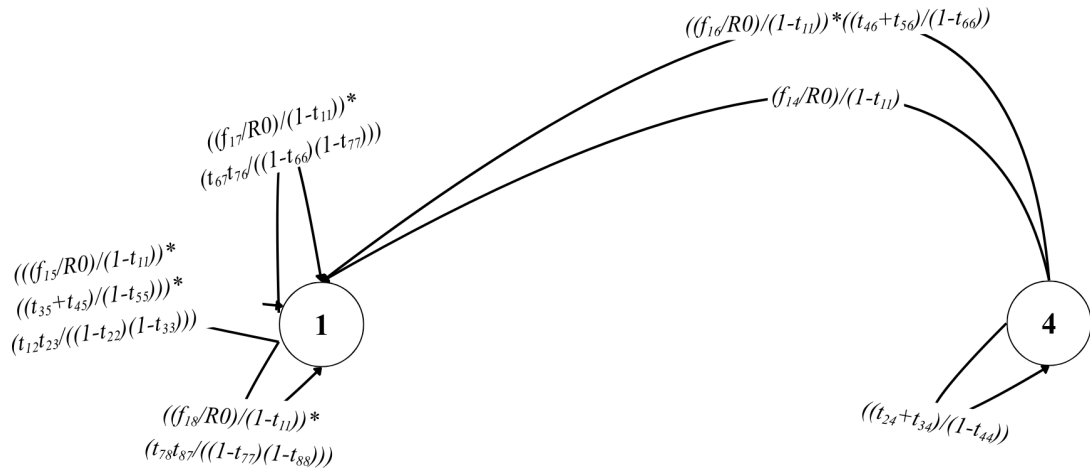
3. Reduce Self-Loops by Rule A



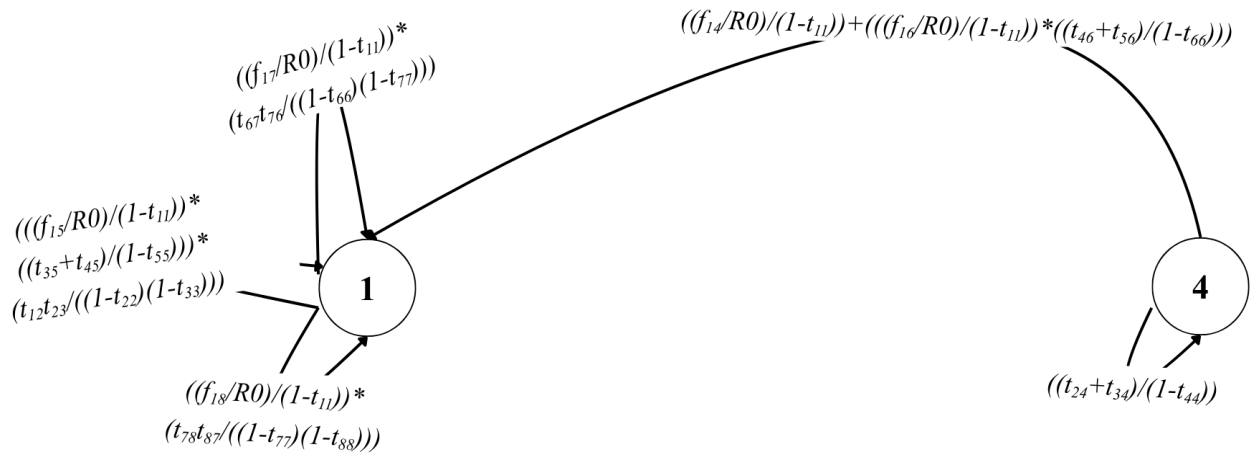
4. Reduce Stage Skips and Backwards Transitions Using Rule B and C



5. Reduce Later-Stage Self-Loops Using Rule C



6. Reduce Fecundity Loops by Rule B



7. Reduce Completely by Rule C

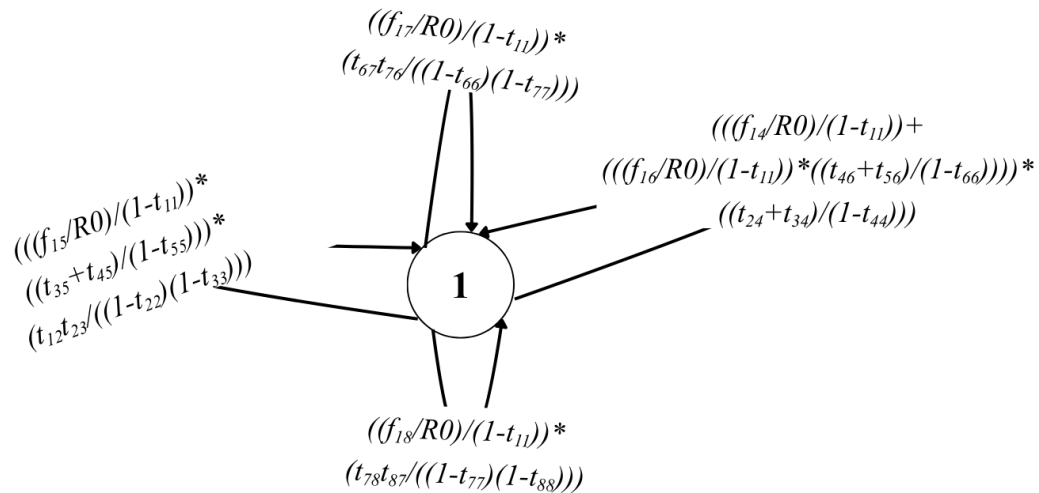


Figure 3: Stepwise graph reduction of *H. rufescens* population matrix. Arrow directions denote transition from one life stage to another. Life stages for abalone were defined by shell size, per the literature. Stage number and shell size associations are described in the Supplemental Materials.

The resulting self-loops were summed and set to 1. After solving for R_0 , we derived the resulting equation, where t terms indicate survivorship probabilities and f terms indicate fecundity contributions:

$$R_0 = \frac{f_{14}(t_{24}+t_{34})}{(1-t_{11})} + \frac{f_{15}t_{12}t_{23}(t_{35}+t_{45})}{(1-t_{22})(1-t_{33})(1-t_{11})(1-t_{55})} + \frac{f_{16}(t_{24}+t_{34})(t_{46}+t_{56})}{(1-t_{22})(1-t_{66})(1-t_{44})} + \frac{f_{17}t_{76}t_{67}}{(1-t_{66})(1-t_{77})(1-t_{11})} + \frac{f_{18}t_{87}t_{78}}{(1-t_{88})(1-t_{77})(1-t_{11})}$$

This function was used as the basis for the R_0 calculation in 3 scenarios outlined below. All further analysis was performed using R programming language in R Studio.

Scenario 1: Varying Harvest Pressure

To illustrate how R_0 could change under different levels of fishing pressure, we amended the baseline function to include a harvest term $(1-H)$, where H is the percent harvested. This adjusted the fecundity contributions for all size classes above the 178 mm legal size limit.

$$R_0 = \frac{f_{14}(t_{24}+t_{34})}{(1-t_{11})} + \frac{f_{15}t_{12}t_{23}(t_{35}+t_{45})}{(1-t_{22})(1-t_{33})(1-t_{11})(1-t_{55})} + \frac{f_{16}(t_{24}+t_{34})(t_{46}+t_{56})}{(1-t_{22})(1-t_{66})(1-t_{44})} + \frac{f_{17}t_{76}t_{67}}{(1-t_{66})(1-t_{77})(1-t_{11})} (1-H) + \frac{f_{18}t_{87}t_{78}}{(1-t_{88})(1-t_{77})(1-t_{11})} (1-H)$$

Scenario 2: Varying Harvest Pressure and Incident Mortality

H. rufescens are hemophilic animals, making them uniquely susceptible to **incident mortality** through cuts incurred by harvest tools. Previous models have defined incident mortality by a 50% decrease in the survivorship of individuals in the size class directly below the legal limit (Rogers-Bennett & Leaf, 2006). This model amended the equation used in Scenario 1 to account for the 50% decrease in survivorship.

$$R_0 = \frac{f_{14}(t_{24}+t_{34})}{(1-t_{11})} + \frac{f_{15}t_{12}t_{23}(t_{35}+t_{45})}{(1-t_{22})(1-t_{33})(1-t_{11})(1-t_{55})} + (0.5) \frac{f_{16}(t_{24}+t_{34})(t_{46}+t_{56})}{(1-t_{22})(1-t_{66})(1-t_{44})} + \frac{f_{17}t_{76}t_{67}}{(1-t_{66})(1-t_{77})(1-t_{11})} (1-H) + \frac{f_{18}t_{87}t_{78}}{(1-t_{88})(1-t_{77})(1-t_{11})} (1-H)$$

Scenario 3: Varying Harvest Pressure and Incident Mortality Under Marine Heatwave Conditions

Marine heatwaves (MHWs) are becoming increasingly prevalent in coastal Pacific waters (Oliver, Donat, & Burrows, et al, 2018). MHWs have led to historic kelp die-offs, resource limitations, and phase shifts in temperate marine ecosystems (McPherson, Finger & Houskeeper, 2021; Rogers-Bennett, Kawana & Catton, 2024). To model MHWs, past work has decreased *H. rufescens* survivorship by 50% across all size classes, modelled growth rate change due to resource limitation by

removing skips in size classes, and decreased fecundity outputs by 1000x (Rogers-Bennett & Leaf, 2006). To mimic this, survivorship for all t terms was multiplied by 0.5, and all f terms were divided by 1000 before being input into the function outlined in Scenario 2.

Strengths and limitations of the model, data, and study

As previously mentioned, our modelling approach was defined by the lack of publicly available data. The matrix on which the above models are based was published in 2006. Due to the temporal sensitivity and data intensity of matrix models, the survivorship values, fecundities, and transitions are likely no longer applicable to modern North Coast *H. rufescens* populations.

Regardless, the use of graph reduction to calculate R_0 of *H. rufescens* populations is a novel application. The derivation and calculation of the R_0 equation can serve as a clear proxy for λ without requiring a dominant eigenvalue or survey-level population information beyond what is needed to construct the matrix. Here, model perturbations were informed by previous, peer-reviewed matrix model studies. Methods from Rogers-Bennett & Leaf were replicated using an R_0 equation. Although the data used are likely no longer applicable in the modern day, replicating such methods from a novel perspective can set a precedent for the use of graph reduction and R_0 calculation in future analyses of *H. rufescens* populations. As will be discussed in the next section, the alignment of survey data with visualized R_0 variation across perturbations can tell an important story about the continued decline of *H. rufescens* populations and provide a framework for investigations to inform historical management trends and future management strategies.

Findings and Discoveries

As previously mentioned, *H. rufescens* has historically been harvested throughout California as an iconic seafood staple for many cultures. Due to a myriad of factors, the recreational *H. rufescens* fishery in Northern California, the last vestige of *H. rufescens* harvesting in the state, closed in 2018. In the R_0 calculations for red abalone, we explored three main scenarios: R_0 of *H. rufescens* with varying harvest pressure, R_0 with varying harvest pressure and incident mortality, and R_0 with varying harvest pressure and incident mortality under MHW conditions (Figure 4). Per the literature, incident mortality is defined as a 50% decrease in survivorship of the size class directly before legal limits in California (150mm - 178mm). This is significant as abalone are normally fished by the insertion of a large abalone ‘iron’ between their foot and the substrate they reside on. This could result in potentially lethal

lacerations to the abalone, which are known to suffer from varying levels of hemophilia. Although newer lab-based research suggests laceration-based mortality may be less than previously assumed (Loeher & Moore, 2020) incidental harvest of near legal abalone and their potential mortality was included in this model to maintain consistency across previous modelling work and explore the effect survivorship decrease of the most elastic size-class (Rogers-Bennet & Leaf, 2006) had on a calculated R_0 . The marine heat wave, in the context of *H. rufescens* life history matrix, is defined as a 50% decrease in all size-class survivorship, the removal of all size-class skips between surveys, and a 1000x decrease in fecundity due to the near-complete loss of macro-algal nutrients (Rogers-Bennett & Leaf, 2006).

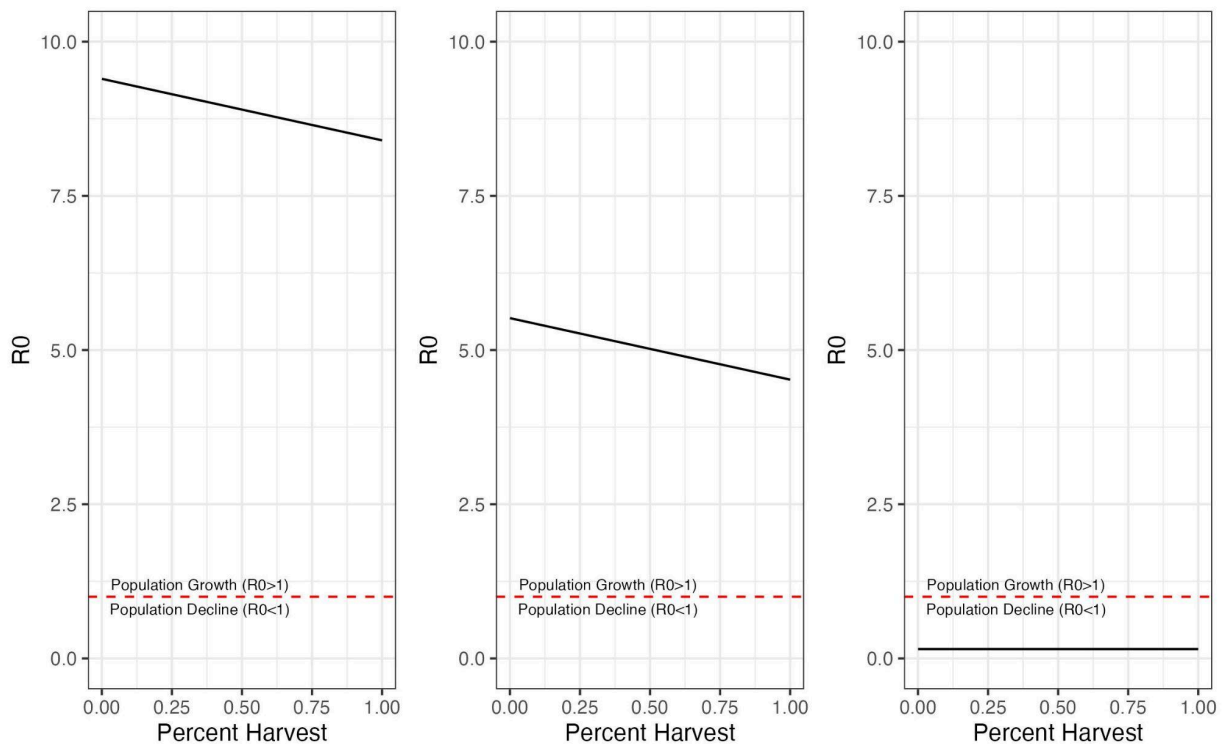


Figure 4: R_0 calculations under 3 different scenarios. Scenario 1 (left) modelled R_0 under varying harvest pressure. Scenario 2 (middle) considers varying harvest pressure, assuming a 50% survivorship decrease in the size class directly below legal size due to incidental fishing mortality. Scenario 3 (right) models R_0 with varying harvest pressure, assuming incident mortality under MHW conditions. The dotted red line denotes the R_0 threshold value ($R_0=1$).

Results suggest that under standard harvest pressure and incident-mortality scenarios, R_0 for *H. rufescens* is above 1, indicating that even under high harvest pressure on the Northern California population, abalone populations are still expected to increase. However, when marine heat waves are incorporated into our modelling, the R_0 of *H. rufescens* is below 1, indicating a steep population

decline regardless of harvest pressure. This suggests that in Northern California, *H. rufescens* population growth is much more limited by marine heat wave events than by recreational fishing pressure.

This data was compared to recent surveys from numerous Northern California study sites, of which we analyzed four: Fort Ross State Park, Point Arena, Point Cabrillo, and Van Damme State Park (Figure 5). In each survey, a drastic decrease in abalone counts was observed after each marine heat wave, compared to years with only standard harvest pressure and incidental harvest (Figure 6). With the recent closure of the abalone fishery, there has yet to be a marked increase in population size. This is likely due to their main food source, *Nereocystis luteana* (bull kelp), struggling to recover to pre-2014 heatwave levels.

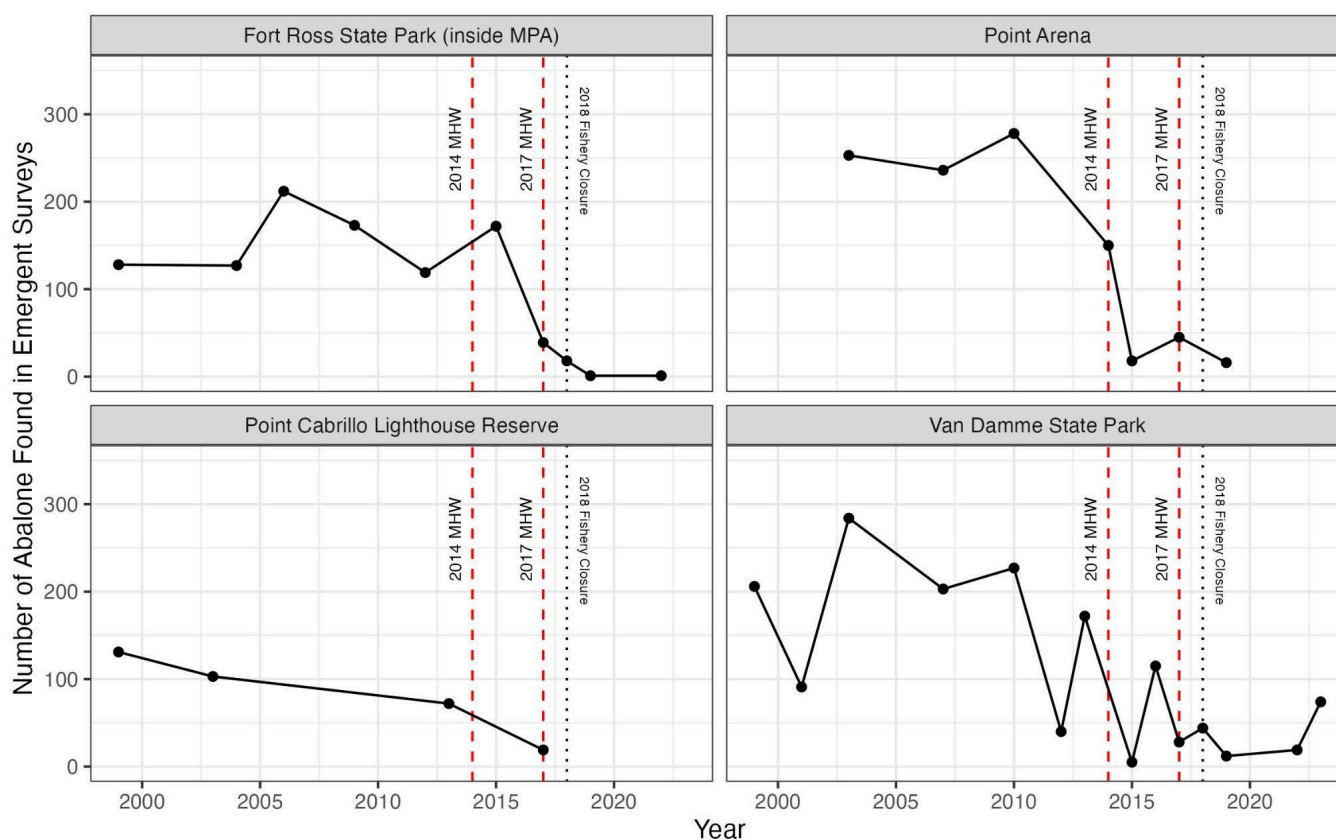


Figure 5: Number of abalone found in emergent surveys from 1999 to 2023 at 4 sites in Northern California. Point data signifies real survey data, while the smooth line represents trends. Red dashed vertical lines indicate MHW events in 2014 and 2017. The dotted black line represents the 2018 recreational fishery closure.

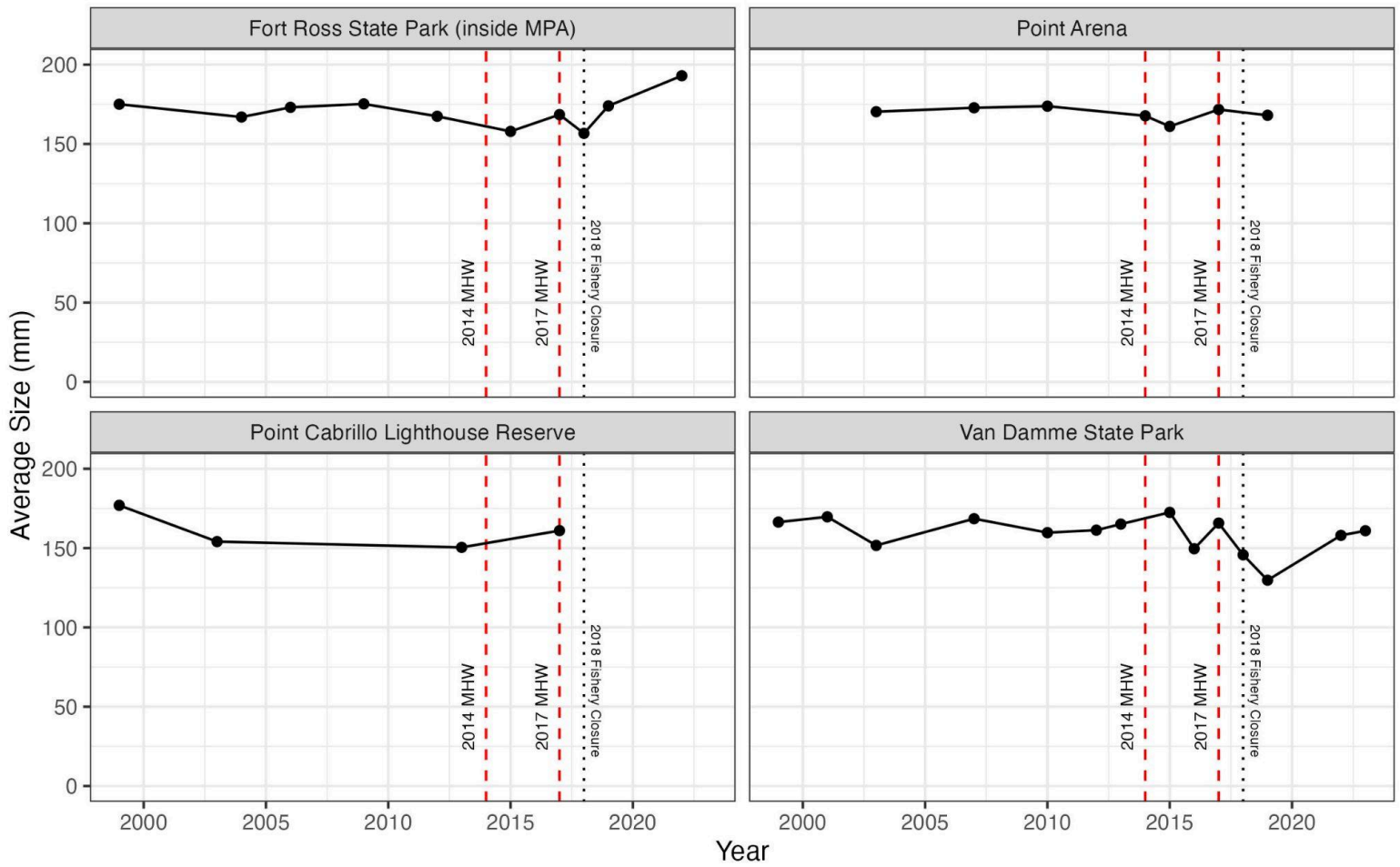


Figure 6: Average size (mm) of abalone found in emergent surveys from 1999-2023 at 4 sites in Northern California. Point data signifies real survey data, while the smooth line represents trends. Red dashed vertical lines indicate MHW events in 2014 and 2017. The dotted black line represents the 2018 recreational fishery closure.

What is the story?

California red abalone have been the subject of intense fishing pressure for centuries. However, the idea that fishing pressure alone is to blame for the current drastic decline of populations throughout the state would not tell the whole story. Red abalone were the unfortunate recipients of a perfect storm of decline from simultaneous ecological stressors. In 2014, a strong marine heatwave known as the Blob swept through the state, facilitating large-scale kelp collapse of the two predominant canopy-forming species of kelp in California, *Macrocystis pyrifera* and *Nereocystis lutea*, the main food of California red abalone. Simultaneously, competitors for this resource, the urchin *Strongylocentrotus purpuratus*, increased in abundance because their main predator, the sunflower sea star *Pycnopodia helianthoides*, populations dropped by ~95% due to sea star wasting disease. This release of predation and lack of canopy-forming kelp resulted in *S. purpuratus* shifting the stable state of many Northern California bull kelp forests to urchin barrens. This shift reduces *H. rufescens* survivorship by reducing the availability of suitable habitat and food resources. Allee effects, in which small population sizes or low densities lead to reduced individual fitness and lower per capita population growth rates, have made recovery difficult for *H. rufescens*, and estimates indicate an 85% decline in the Northern California population, prompting a full shutdown of the recreational fishery. The calculated R_0 under 1 (0.151) describes this decline quantitatively.

There is cautious optimism regarding the recovery of *H. rufescens*, as reflected in the R_0 values of the two other harvest scenarios. If factors conducive to the success of *H. rufescens* are restored to pre-marine heatwave conditions, as illustrated by a shift towards a bull kelp-dominated stable state, the R_0 suggests that recovery could be achieved due to the effectiveness of broadcast spawning across multiple size classes, regardless of fishing pressure or incident mortality. However, Allee effects, which are not studied in this chapter, may detract from population growth modelled by R_0 calculations, mirroring the above methods. Regardless, this conclusion underscores the importance of and the interconnectedness between current and future bull kelp recovery activities in Northern California and the persistence of abalone populations.

The return of recreational abalone fishing in Northern California would bring a projected \$44M to the local economy. In towns like Fort Bragg and Mendocino, many businesses have not been able to recover due to the loss of the abalone fishing season. The area's only dive shop shuttered its doors after the loss of divers coming to harvest abalone, removing the only publicly available SCUBA cylinder compressor in the area. The return of recreational fishing for *H. rufescens* would likely bring a revitalization not only of Northern California marine community assemblages but also of the coastal human communities that live adjacent to them.

Next Steps and Further Considerations

The life history matrix used in this study was based on survivorship from 2006 data. Updating the transition probabilities with post-2014 marine heatwave survivorship data would dramatically increase the model's relevance to the 2036 reopening decision. It is hoped that this graphical reduction of the 2006 data can be used for further synthesis and provide the basis for conducting this analysis in the future. Furthermore, attaching a spatial component to this data set could be a logical next step.

Understanding site-specific R_0 could help managers of the *H. rufescens* create experimental re-openings of the recreational fishery where there is accurate data on kelp availability, local density estimates and survivorship.

The experimental harvest pressure scenarios could be expanded to include tiered catch limits, smaller bag limits, or different permit systems. This analysis would help inform CDFW policy and regulation post-opening in 2036. Furthermore, these differing harvest pressure scenarios could be coupled with kelp recovery projections to make the chapter directly actionable for managers. In this case, one scenario could assume continued kelp suppression while the other assumes a meaningful kelp recovery.

Lastly, exploring Allee effects in more detail would provide managers with a benchmark for evaluating readiness to reopen. Identifying the specific density of *H. rufescens* below which successful external fertilization becomes unlikely would provide the basis for a threshold to be created independent of R_0 . For example, R_0 could be high with the population still too sparsely distributed locally for reproduction to succeed. Thus, having this information would paint a more accurate picture of abalone recovery in Northern California.

Declaration of AI Use

During the preparation of this chapter, the authors used Grammarly, version 1.155.0.0, for text editing and Anthropic's Claude and Claude Code for troubleshooting R coding errors. The authors have reviewed and edited the output and take full responsibility for the content of this publication.

Acknowledgments

We would like to extend a huge thank-you to Professor Chris Jerde for his guidance throughout this project. Without his support, there may not have been a graphical reduction of the life history transition stages of *Haliotis rufescens*. Although not used in this chapter's analyses, the authors would like to extend special thanks to Ian Kelmartin at the California Department of Fish and Wildlife for

providing survey data for future directions. Finally, we would like to thank Dr. Laura Rogers-Bennett for her unending research efforts to protect California's abalone and the larger marine environment.

References

- Ault, J. S. (1985). Species Profiles. Life Histories and Environmental Requirements of Coastal Fishes and Invertebrates (Pacific Southwest). Black, Green, and Red Abalones.
- Braje, T.J., Erlandson, J.M., Rick, T.C., Dayton, P.K. and Hatch, M.B.A. (2009). Fishing from past to present: continuity and resilience of red abalone fisheries on the Channel Islands, California. *Ecological Applications*, 19. 906-919. <https://doi.org/10.1890/08-0135.1>
- California Department of Fish and Game (2010). Abalone Recovery and Management Plan Status Report - Northern California Red Abalone Fishery.
<https://nrm.dfg.ca.gov/FileHandler.ashx?DocumentID=29511&inline>
- California Department of Fish and Game (2003). Annual Status of the Fisheries Report: Abalones.
<https://nrm.dfg.ca.gov/FileHandler.ashx?DocumentID=34381&inline>
- California Department of Fish and Wildlife, Catton, C., Rogers-Bennett, L. (2016). "Perfect Storm" Decimates Northern California Kelp Forests. *Marine Management News*.
<https://cdfwmarine.wordpress.com/2016/03/30/perfect-storm-decimates-kelp/>
- California Department of Fish and Wildlife (2025). News Release: California Fish and Game Commission Extends Red Abalone Recreational Fishery Closure.
<https://wildlife.ca.gov/News/Archive/california-fish-and-game-commission-extends-red-abalone-recreational-fishery-closure-finds-cesa-listing-of-bear-lake-buckwheat-warranted>
- Caswell, H. (2001). *Matrix Population Models: Construction, Analysis, and Interpretation* (2nd Edn.). Sinauer Associates, Sunderland, MA.
- Caswell, H. (2019). *Sensitivity Analysis: Matrix Methods in Demography and Ecology*. Springer Cham.
<https://doi.org/10.1007/978-3-030-10534-1>
- de-Camino-Beck, T., Lewis, M. A. (2008). On Net Reproductive Rate and the Timing of Reproductive Output. *The American Naturalist*, 172(1), 128-139.
<http://www.jstor.org/stable/10.1086/588060>

- Jones, O.R. (2026). Matrix Population Modelling. In O.R. Jones (Ed). *BB512: Population Biology and Evolution*. University of South Denmark. https://jonesor.github.io/BB512_Book/index.html
Accessed 19 March, 2026.
- Loeher, M.M. & Moore, J.D. (2020). Foot injury survival in red abalone (*Haliotis rufescens*). *Aquaculture*, 529(15). <https://doi.org/10.1016/j.aquaculture.2020.735734>
- McPherson, M.L., Finger, D.J.I., Houskeeper, H.F. et al. (2021). Large-scale shift in the structure of a kelp forest ecosystem co-occurs with an epizootic and marine heatwave. *Community Biology*, 4, 298. <https://doi.org/10.1038/s42003-021-01827-6>
- Reid, J., Rogers-Bennett, L., Vásquez, F., Pace, M., Catton, C. A., Kashiwada, J. V., & Taniguchi, I. K. (2016). The economic value of the recreational red abalone fishery in northern California. <http://hdl.handle.net/11447/2161>
- Rogers-Bennett, L., Dondanville, R. F., Catton, C. A., Juhasz, C. I., Horii, T., & Hamaguchi, M. (2016). Tracking Larval, Newly Settled, and Juvenile Red Abalone (*Haliotis rufescens*) Recruitment in Northern California. *Journal of Shellfish Research*, 35(3), 601-609. <https://doi.org/10.2983/035.035.0305>
- Rogers-Bennett, L., Hubbard, K. E., & Juhasz, C. I. (2013). Dramatic declines in red abalone populations after opening a “de facto” marine reserve to fishing: Testing temporal reserves. *Biological Conservation*, 157, 423-431. <https://doi.org/10.1016/j.biocon.2012.06.023>
- Rogers-Bennett, L., Kawana, S. K., Catton, C. A., Klamt, R., Dondanville, R., Maguire, A., & Okamoto, D. K. (2025). Abalone recruitment patterns before and after sea urchin barrens formation in northern California: incorporating climate change. *New Zealand Journal of Marine and Freshwater Research*, 59(1), 283–299. <https://doi.org/10.1080/00288330.2024.2403596>
- Rogers-Bennett, L., Leaf, R. T. (2006). Elasticity analyses of size-based red and white abalone matrix models: Management and conservation. *Ecological Society of America: Ecological Applications*, 16(1), 213-224. <https://doi.org/10.1890/04-1688>
- Rogers-Bennett, L., Rogers, D. W., & Schultz, S. A. (2007). Modeling Growth and Mortality of Red Abalone (*Haliotis rufescens*) in Northern California. *Journal of Shellfish Research*, 26(3), 719–727. [https://doi.org/10.2983/0730-8000\(2007\)26%255B719:MGAMOR%255D2.0.CO;2](https://doi.org/10.2983/0730-8000(2007)26%255B719:MGAMOR%255D2.0.CO;2)
- Virgin, S. D. S., Gerrity, S., & Schiel, D. R. (2025). Recreational fishing effects on New Zealand abalone (pāua, *Haliotis iris*) after five years of fishery closure: a matrix-based approach. *Marine Environmental Research*, 210, 107276. <https://doi.org/10.1016/j.marenvres.2025.107276>

Supplemental materials

Supplemental Table 1: Associations of graphed life stages with corresponding size classes.

Life Stage	Size Class (mm)
1	25-50
2	50.1-75
3	75.1-100
4	100.1-125
5	125.1-150
6	150.1-178
7	178.1-200
8	>200

R₀ Modelling Code:

```
# Matrix Modeling Data Poor Fisheries
# study organism: Red Abalone
# Study area: Sonoma and Mendocino Counties, CA
# Eva Juengling Bean, Daniel O'Shea
# ESM 211
# created: 2/25/2026
# last modified: 3/13/2026
#####
rm(list=ls())
# load libraries
library(tidyverse)
library(here)
library(janitor)
library(ggplot2)
library(popbio)
library(patchwork)
# define variables
t11 <- 0.191
t12 <- 0.191
t22 <- 0.045
t23 <- 0.36
t24 <- 0.045
t33 <- 0.148
```



```

labs(x="Percent Harvest", y="R0")+
theme_bw()
harvest_plot
# function with varying harvest assuming incident mortality
harvest_incident_r0 <- function(H){
  ((f14*(t24+t34))/(1-t11))+((t12*t23*f15*(t35+t45))/((1-t22)*(1-t33)*(1-t11)*(1-t55)))+
  ((0.5)*((f16*(t24+t34)*(t46+t56))/((1-t11)*(1-t66)*(1-t44)))+((1-H)*((t76*t67*f17)/((1-t66)*(1-t77)*(1-t11))))+
  ((1-H)*((t87*t78*f18)/((1-t11)*(1-t77)*(1-t88))))
}
r0_incident <- harvest_incident_r0(harvest) # using harvest vector from above, run function for new r0 values
harvest_incident_df <- data.frame(x=harvest, y=r0_incident) # create new data frame
# plot!
incident_plot <- ggplot(harvest_incident_df, aes(x=harvest, y=r0_incident))+
  xlim(c(0,1))+
  ylim(c(0,10))+
  geom_line()+
  geom_hline(yintercept=1, color="red", linetype="dashed")+
  annotate("text", x=0.35, y=1.2, size=2.5, label="Population Growth (R0>1)")+
  annotate("text", x=0.35, y=0.8, size=2.5, label="Population Decline (R0<1)")+
  labs(x="Percent Harvest", y="R0")+
  theme_bw()
incident_plot
# function for r0 with varying harvest assuming incident mortality and MHW conditions
# first have to adjust matrix values based on Rogers-Bennett & Leaf, 2006
t11_adj <- 0.191*0.5 # all survivorship decreased by 50%
t12_adj <- 0.191*0.5
t22_adj <- 0.045*0.5
t23_adj <- 0.36*0.5
t24_adj <- 0 # indicated no size stage skips
t33_adj <- 0.148*0.5
t34_adj <- 0.342*0.5
t35_adj <- 0
t44_adj <- 0.18*0.5
t45_adj <- 0.405*0.5
t46_adj <- 0
t55_adj <- 0.321*0.5
t56_adj <- 0.343*0.5
t66_adj <- 0.67*0.5
t67_adj <- 0.06*0.5
t76_adj <- 0.048*0.5
t77_adj <- 0.726*0.5
t78_adj <- 0.01*0.5
t87_adj <- 0.01*0.5
t88_adj <- 0.735*0.5
f14_adj <- 0.8/1000 # all fecundity decreased 1000x
f15_adj <- 3.79/1000
f16_adj <- 12.33/1000
f17_adj <- 24.02/1000
f18_adj <- 30.33/1000
harvest_MHW_r0 <- function(H){
  ((f14*(t34_adj))/(1-t11_adj))+((t12_adj*t23_adj*f15_adj*(t45_adj))/((1-t22_adj)*(1-t33_adj)*(1-t11_adj)*(1-t55_adj)))+
  ((0.5)*((f16_adj*(t34_adj)*(t56_adj))/((1-t11_adj)*(1-t66_adj)*(1-t44_adj)))+((1-H)*((t76_adj*t67_adj*f17_adj)/((1-t66_adj)*(1-t77_adj)*(1-t11_a
  dj))))+
  ((1-H)*((t87_adj*t78_adj*f18_adj)/((1-t11_adj)*(1-t77_adj)*(1-t88_adj))))
}
r0_MHW <- harvest_MHW_r0(harvest) # new r0 values from function!

```

```
harvest_MHW_df <- data.frame(x=harvest, y=r0_MHW) # new data frame!  
# plot!  
MHW_plot <- ggplot(harvest_MHW_df, aes(x=harvest, y=r0_MHW))+  
  xlim(c(0,1))+  
  ylim(c(0,10))+  
  geom_line()+  
  geom_hline(yintercept=1, color="red", linetype="dashed")+  
  annotate("text", x=0.35, y=1.2, size=2.5, label="Population Growth (R0>1)")+  
  annotate("text", x=0.35, y=0.8, size=2.5, label="Population Decline (R0<1)")+  
  labs(x="Percent Harvest", y="R0")+  
  theme_bw()  
MHW_plot  
# create composite plot using patchwork package  
composite_r0 <- harvest_plot+incident_plot+MHW_plot  
composite_r0
```